Journal Name

COMMUNICATION

Facile fabrication of structure tunable bead-shaped hybrid microfibers by a Rayleigh instability guiding strategy

Received 00th January 20xx,
Accepted 00th January 20xx

DOI: 10.1039/x0xx00000x

www.rsc.org/

Yan Zhang, † Yu Tian, † Ling-Ling Xu, Cai-Feng Wang, and Su Chen*

A method allowing fabrication of quantum-dots or photonic crystals loaded bead-shaped hybrid microfibers arrays in a Rayleigh instability driven drop-sliding manner is demonstrated.

One-dimensional (1D) heterostructured microfibers are greatly promising for the achievement of anisotropic geometric features, unique physicochemical properties and functionalities. Especially, bead-shaped microfibers with alternate beads and strings structures have received increasing attention in recent years because of their unique applications in photoelectric and biomimetic fields, as well as their use as sensors.[1-4] To date, several methods for fabricating bead-shaped 1D microstructures have been rationally investigated, such as self-assembly,[5] electrospinning methods,[6] and microfluidic spinning.[7] Jiang's group developed a Rayleigh instability driven wet-rebuilt strategy and a electrospinning/electrospraying combined strategy to generate periodic bead-shaped fibers for water-collecting application.[8-10] Lee's group obtained artificial fibers with controllable spindle-knots and joints using a microfluidic system consisting of a digital and programmable flow control.[11] Qin's group reported the preparation of biomimetic bamboo-like microscale hybrid fibers with multiple functionalities by combining the droplet microfluidic technique with the wet-spinning process.[12] Despite obvious progress, most of the reported methods employed either advanced equipment, harsh experimental conditions or complex operations, thereby limiting the extensive applications of heterostructured materials. Therefore, it should be of great significant to explore a simple yet feasible approach toward developing 1D heterostructured materials with unique properties and functionalities.

Here, we propose a simple and facile method enabling quantum-dots (QDs) chemical reaction and photonic crystals (PCs) precursor physical assembly to bead-shaped microfibers. The method is based on a Rayleigh instability driven drop-sliding principle combined with a spinning process, which allows large drops to slide along the microfiber, and then to continuously break up into ordered droplets, forming well-defined microfibers with alternate beads and strings structure. For an example, when a large drop containing sulfur ions slides to the PVP microfiber containing Cd^{2+}, the beads of CdS QDs with high fluorescence were *in-situ* formed along the microfiber during the process of spinning. On a second example, when a large drop containing monodispersed polystyrene (PS) colloid particles or carbon quantum dots (CQDs) slide to the PLA microfiber, the beads of PS PCs or fluorescent CQDs were then right away obtained onto the microfiber. This finding offers a new insight into bead-shaped microfiber arrays and might open a promising avenue to fundamental research.

Rayleigh instability involves a falling stream of fluid breaking up into smaller droplets with almost the same volume but less surface area (Fig. S1, ESI†). This driving force of the Rayleigh instability allows liquids, by virtue of their surface tensions, to tend to minimize their surface area.[13,14] In this case, in fabrication of these Rayleigh instability driven bead-shaped microfibers (RDBFs), we chose the polymer fiber as a carrier and drops as a sliding liquid phase. The drops break up into ordered discrete droplets by aid of gravity and surface forces, and then load on the surface of the microfibers. With the evaporation of solvent, the physical and chemical interactions between the droplets and fibers prompt the formation of bead-shaped hybrid microfibers (Scheme 1a). By introducing different building blocks into sliding liquid phase, we successfully achieved a series of bead-shaped microfibers with multilevel microstructures and varied chemical compositions. Observed from the cross-section, these 1D multisegmented bead-shaped microfibers were classified into three main structural categories including a cylindrical solid microstructure, a one-shell microstructure and a two-shell microstructure (Scheme 1b). Illuminatingly, through applying

State Key Laboratory of Materials-Oriented Chemical Engineering and College of Chemistry and Chemical Engineering. NanjingTech University (former Nanjing University of Technology), 5 Xin Mofan Road, Nanjing 210009, P. R. China.
E-mail: chensu@njtech.edu.cn
† These authors contributed equally.
‡ Electronic Supplementary Information (ESI) available: materials, experimental section, characterization and additional figures. See DOI: 10.1039/x0xx00000x

different liquid-solid system, RDBFs can be designed into various compositional and structural microfibers in a highly controllable manner, which may provide potential possibility to construct bead-shaped microfibers with predefined microstructures.

Microreactors have drawn much attention due to their high reaction efficiency, energy conversation and environmental friendly advantage. Much effort has been developed to the construction of microreactors on the basis of droplets,[15] fiber knot,[16] films,[17] microspheres,[18] and the template method.[19] Innovatively, this liquid-solid system could also be applied as a 0D–1D dot-line contact reactor platform by introducing reactants into the fiber and drop phases, respectively. At the intersections between the base microfiber and sliding droplets phase, ultrasmall-volume reactors were constructed, meanwhile, hybrid microfibers with unique optical properties and microstructures were also generated. More importantly, by combining the RDBFs with a spinning technology, we successfully realized the formation of fluorescent microarrays. As shown in Scheme 1c, we introduced syringe pump to drive the high concentration of polymer phase outside. A uniform polymer fiber (with 150 μm diameter) was directly received by a spinning receiver equipment. After straightening a polymer microfiber at vertical direction (length = 30 cm), a drop of liquid from the exit tip of microchannel (d = 1.2 mm) was placed on the middle of polymer fiber, allowing the upper discrete droplets had enough time to reach steady state before being taken into array and the new beads forming, simultaneously. The relations of microfiber diameters and motor speed refer to the reported literature, and the space of the fibers is a function of the rotating motor speed (Fig. S6 and S7, ESI †).[16b] Through the optimization of the process parameters, the flow velocity of the polymer phase and the rotating motor speed were fixed at 0.1 $mL \cdot h^{-1}$ and 10 $rad \cdot min^{-1}$, respectively.

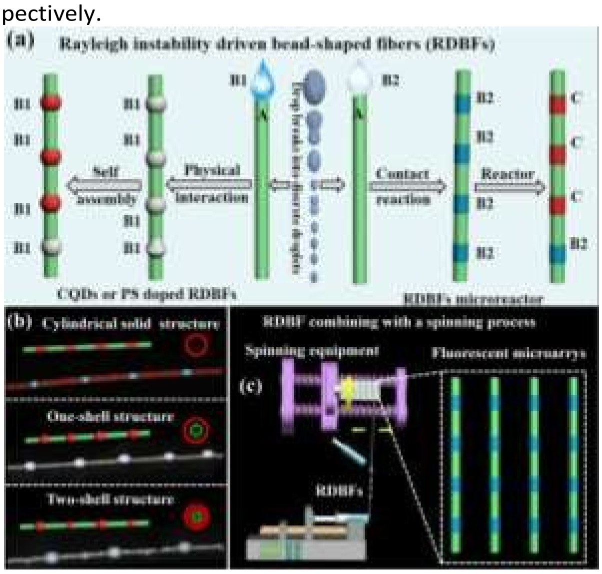

Scheme 1 (a) Schematic diagram of evolution of the drop based on Rayleigh instability and the fabrication route to form Rayleigh instability driven bead-shaped fibers (RDBFs). (b) Three different structures of RDBFs observed from the cross-section: cylindrical solid microstructure, one-shell microstructure and two-shell microstructure. (c) RDBFs arrays fabricated via a spinning process.

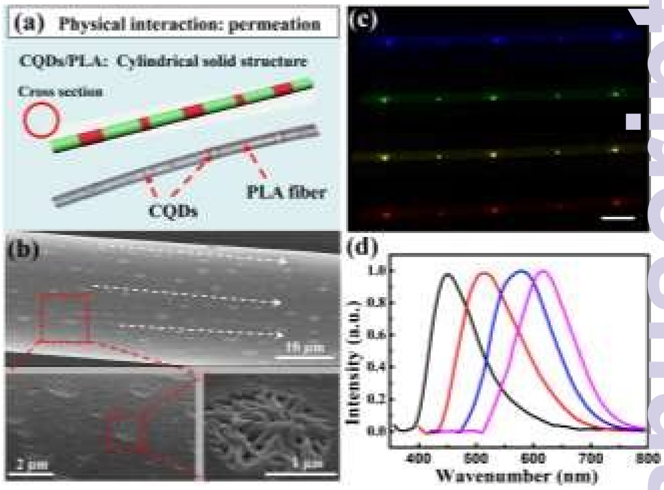

Fig. 1 (a) Schematic diagram of CQDs doped RDBFs with cylindrical solid microstructure. (b) Low and high magnification SEM images of as prepared CQDs doped RDBFs. (c) Fluorescent micrographs of CQDs doped RDBFs at excitation of 365nm, 395 nm, 453 nm and 535 nm from top to bottom, respectively (scale bar = 1 mm). (d) Normalized PL intensities of fluorescent CQDs doped RDBFs corresponding to the samples of blue, green, yellow and red CQDs, respectively.

Fig. 1 shows an example of carbon quantum dots (CQDs) carried out in microfiber beads. We chose water-soluble CQDs sliding phase and oil soluble PLA polymer microfiber. As shown in Fig. 1a and S2, ESI†, the CQDs loaded drop broke up into ordered beads along the PLA microfiber, and CQDs/PLA hybrid microfibers with alternate beads and strings microsturctures were formed. They display a cylindrical solid microstructure because that CQDs solution penetrated into the pore structure of microfiber (Fig. 1b). We further explored the fluorescent properties of CQDs/PLA hybrid fibers. Fig. 1d shows a typical excitation dependent feature that the maximum emission peak shifts to longer wavelengths as the excitation wavelength increases, similar to those previously reported.[20, 21] At 365 nm, 395 nm, 453 nm and 535 nm excitation wavelength, the CQDs/polymer hybrid microfibers exhibit bright periodic blue, green, yellow and red fluorescence patterns (Fig. 1c), respectively, with the corresponding maximum PL emission band at 438, 496, 57[illegible] and 600 nm (Fig. 1d), respectively. The results demonstrate the CQDs nanoparticles transferred to PLA microfibers matrix could maintain well fluorescent property. More importantly, the resulting hybrid polymer microarrays with alternative fluorescent patterns may offer a new avenue to construction of multisegmented configuration, presenting a variety of applications, such as fluorescent codes and displays. In the following work, we have made efforts to achieve hybrid microfibers with coded fluorescence. As shown in Fig. S3, ESI †, by introducing red fluorescent dyes into PLA polymer microfibers, bead-shaped hybrid microfibers with alternative blue and red fluorescence patterns were obtained. The above results demonstrate the simplicity and flexible controllability of this strategy for the successful generation of bead-shaped QDs/polymer hybrid microfibers with encoded fluorescence, which might facilitate the fluorescent codes and display research.

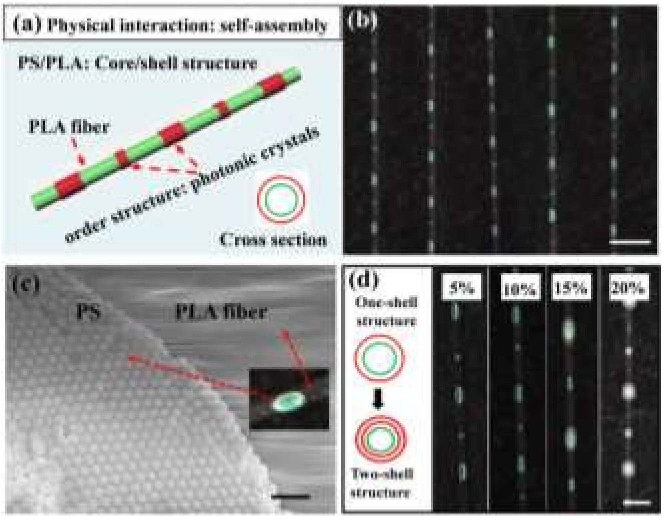

Fig. 2 (a) Schematic diagram of PS doped RDBFs with a core/shell microstructure. (b) Optical micrographs of PS doped RDBFs array constructed by PS microspheres with diameter of 290 nm (scale bar = 1mm). (c) SEM image of the as-obtained PS doped RDBFs (scale bar = 1μm). (d) Optical micrographs of PS doped RDBFs under different PS concentrations: 5%, 10%, 20% and 30% along with the changing structure (scale bar = 500 μm).

The second set of experiments was focused on PS PCs loaded RDBFs. By introducing PS microspheres into the sliding liquid phase, we obtained bead-shaped microfibers with different microstructures and functionalities. Due to the diameter of PS microspheres larger than pore structure of the polymer fiber, the PS microspheres just loaded on the microfiber surface forming core/shell microstructure (Fig. 2a). With the solvent evaporation, these PS microspheres self-assembled into order structure constructing so-called photonic crystals (PCs) and exhibited brilliant structural colors on the surface of PLA polymer fibers (Fig. S7, ESI†).[22a,b] By combing with the spinning technique and using of the PS microspheres with diameters of 290, 320 nm, we successfully obtained the green and red microarrays of these PS/PLA RDBFs, which the corresponding reflection peaks located at 578 and 605 nm, respectively (Fig. 2b and S4, ESI†). To verify the existence and distribution of PS microspheres on the microfibers, we further observed the morphology of PS/PLA microfibers by SEM. We can obviously observe from Fig. 2c that the microspheres are spherical with smooth surface and are highly monodispersed and ordered. As these unique colors (opalescence) originate from the physical structure, they can endure photo-irradiation, chemical compounds or electrical and magnetic fields, which could be extendable to sensor and display fields.[22c]

These multisegmented micromaterials are attractive not only because of their unique optical properties, but also for their fantastic architectures. Based on the special core/shell mcirostructures, we further explored the effect of PS concentration on the morphology of bead-shaped hybrid microfibers. As the volume of PS sliding phase and the length of PLA microfiber were fixed, the distance between the beads remain unchanged in falling process. It is clear that the morphology of the PS/PLA microfibers is greatly affected by the shell size of beads. As shown in Fig. 2d and S5, ESI†, at a low concentration of 5%, the bead-shaped hybrid microfibers present one-shell microstructures. With the increase of the PS concentration, they has been gradually transformed into multi-shell microstructures with larger shell diameters. We assume that this might be caused by the following reasons. The increase in concentration leads to gains in viscosity of sliding droplet phase, meanwhile, the surface tension of the PS suspensions and the friction force between the droplet and PLA polymer microfibers increase with the increasing concentration of PS. As a result, the PS sliding phase gradually broke up into pearly bead with larger size and bead-shaped microfibers with multi-shell microstructures were obtained. As we believed, the results imply that an increase of the PS sliding phase concentration significantly increased the bead size along the PLA polymer microfiber with only minor effects on the internal distance between the droplets. It is predicted that the hybrid microfibers containing aligned droplets may be a facile way to produce various functional bead-shaped microfibers with unique physical and chemical properties.

As above, basing on the interface physical interaction between the droplet and the microfibers, we successfully obtained various bead-shaped microfibers with different microstructures and optical properties. To our knowledge, these 1D micromaterials with a larger specific area and additional heterogeneous interfaces also provide an ideal platform for the contact chemistry reaction used for various applications in materials synthesis and analysis. Inspired by the work of Palacios[16a] and our former work[16b] on chemical reactors within fiber junctions, we innovatively extended the liquid-solid system to 0D-1D dot-line contact reactor for the *in situ* fabrication of fluorescent hybrid RDBFs. In this case, the PVP polymer fiber directly drawn from the mixed PVP ethanol solution (30 wt%) with cadmium source (0.2 M Cd^{2+}) was used as a 1D main base-fiber. And then one acetone drop with sodium sulfide (0.2 M S^{2-}) was taken as 0D liquid phase. When 0D droplet sliding phase rolled along the 1D solid fiber, reagents deposited on the ridge areas transferred to the surface (Fig. S8, ESI†) and the reaction of Cd^{2+} and S^{2-} occurred during the solvent evaporation. When the droplets evaporated completely, leaving the CdS nanoparticles compress into bead-liked and segmented microarrays (Fig. 3a). The microfibers with bead-shaped segments show alternative white-yellow color under daylight and dark-yellow fluorescence under 365 nm UV light (Fig. 3b and S8, ESI†). PL spectrum (Fig. 3c) of obtained CdS QDs segments shows a broad peak centered at 550 nm. These bright yellow beads on the fibers actually give a direct view of the heterostructured fluorescent bead-patterned microfibers. Time-resolved photoluminescence measurements indicate that CdS/PVP hybrids have decay lifetimes of 8.80 ± 0.05 ns (Fig. S9, ESI†). The *in-situ* generation of CdS QDs in the polymer matrixes provides CdS/PVP QD-polymer microfibers with good chemical compatibility and favorable fluorescence, which allowing it easy to realize the construction of fluorescent microarrays through 0D-1D microreactors carried out on ultra-small scales and ambient temperature.

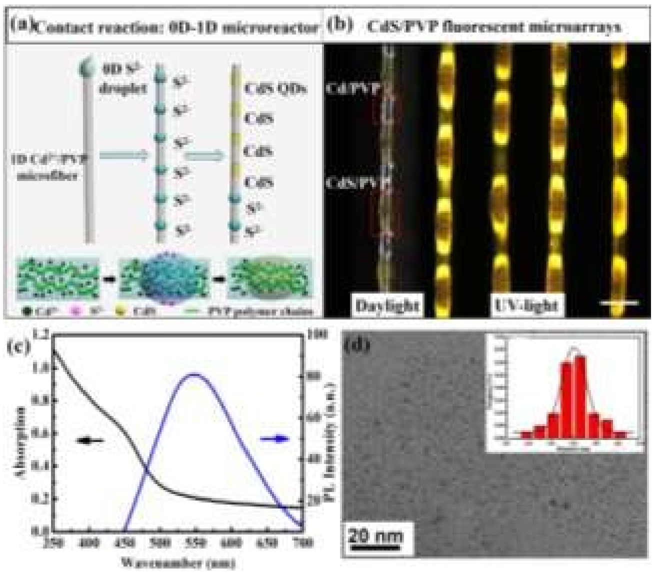

Fig. 3 (a) Schematic diagram of 0D-1D microreactor for *in-situ* fabricating QDs doped RDBFs. (b) Optical micrograph of CdS QDs doped RDBFs under daylight and fluorescent micrograph of CdS QDs doped RDBFs array under UV-light (scale bar = 300 μm). (c) Absorption and PL spectra of CdS QDs. (d) TEM image of CdS QDs embedded in fiber, inset: the particle size distribution.

To further verify the existence and distribution of CdS QDs in the PVP microfibers, transmission electron microscopy (TEM) was employed. In TEM images (Fig. 3d and S10, ESI†), the as-prepared CdS QDs are relatively uniform and well-dispersed without obvious aggregation. The mean size of the CdS QDs was measured to be about 3.5 nm,[23] corresponding to the standards of QDs. The size-distribution diagram and a coefficient of variation (CV) of these nanoparticles of about 12.3% (Table S1, ESI†) further indicates that the QDs have relatively narrow size distribution. By virtue of chemical incorporation between QDs and polymer matrixes, these *in-situ* generated CdS QDs are highly stable without fluorescence quenching over several months (Fig. S11a, ESI†). Due to the particle growth of CdS QDs, PL emission peak exhibits a red shift from 530 nm to 600 nm, while the PL intensity of microfibers is stable at room temperature for over several months with no significant change (Fig. S11b, ESI†). The above results clearly demonstrate the successful synthesis of well-defined CdS QDs in polymer hybrid microfibers, which actually adds versatility to this facile and effective method for construction of various types of reactions and for fabrication of composite hybrid microfibers.

The method is versatile, bead-shaped hybrid microfiber arrays with varied compositional and structural properties can utilize this Rayleigh instability driven drop-sliding principle, along with a spinning technology. Both the CdS QDs or carbon quantum dots and photonic crystals reagents used in this method may yield good examples to fabricate other bead-shaped composite hybrid microfibers. More importantly, we expect that the design may endow the heterostructured materials even more functionalities and robust applications, such as sensors, label analysis and microreactors.

This work was supported by National Natural Science Foundation of China (21076103, 21474052 and 21176122), Priority Academic Program Development of Jiangsu Higher Education Institutions (PAPD), and Qing Lan Project.

Notes and references

1 P. Anzenbacher, F. Y. Li and M. A. Palacios, *Angew. Chem. Int Ed.*, 2012, **51**, 2345.
2 X. L. Tian, H. Bai, Y. M. Zheng and L. Jiang, *Adv. Funct. Mater.*, 2011, **21**, 1398.
3 S. J. Wang, S. L. Feng, Y. P. Hou and Y. P. Zheng, *Macromol. Rapid. Commun.*, 2015, **36**, 459.
4 Y. P. Hou, L. C. Gao, S. L. Feng, Y. Chen, Y. Xue, L. Jiang and Y. M. Zheng, *Chem. Commun.*, 2013, **49**, 5253.
5 S. J. Hurst, E. K. Payne, L. Qin and C. A. Mirkin, *Angew. Chem. Int. Ed.*, 2006, **45**, 2672.
6 J. F. Zheng, A. H. He, J. X. Li, J. A. Xu and C. C. Han, *Polymer*, 2006, **47**, 7095.
7 (a) Y. Jun, E. Kang, S. Chae and S. H. Lee, *Lab. Chip.*, 2014, **14**, 2145; (b) X. B. Ji, S. Guo, C. F. Zeng, C. Q. Wang and L. X. Zhang, *RSC Adv.*, 2015, **5**, 2517; (c) X. H. He, W. Wang, Y. M. Liu, M. Y. Jiang, F. Wu, K. Deng, Z. Liu, X. J. Ju, R. Xie and L. Y. Chu, ACS Appl Mater Interfaces, 2015, 7, 17471; (d) E. Um, J. K. Nunes, T. Picob and H. A. Stone, *J. Mater. Chem. B,* 2014, **2**, 7866.
8 Y. C. Wu, X. Chen, B. Su, Y. L. Song and L. Jiang, *Adv. Funct. Mater.*, 2012, **22**, 4569.
9 H. Bai, R. Sun, J. Ju, X. Yao, Y. Zheng and L. Jiang, *Small*, 2011, **7**, 3429.
10 P. W. Fan, W. L. Chen, T. H. Lee and J. T. Chen, *Macromol. Rapid. Commun.*, 2012, **33**, 343.
11 E. Kang, G. S. Jeong, Y. Y. Choi, K. H. Lee, A. Khademhosseini and S. H. Lee, *Nat. Mater.*, 2011, **10**, 877.
12 Y. Yu, H. Wen, J. Ma, S. Lykkemark, H. Xu and J. Qin, *Adv. Mater.*, 2014, **26**, 2494.
13 (a) G. E. A. Meier, A. Klopper and G. Grabitz, *Exp. Fluids.*, 1992, **12**, 173; (b) M. Tjahjadi, H. A. Stone and J. M. Ottino, *J. Fluid Mech.*, 1992, **243**, 297.
14 J. Eggers, *Rev. Mod. Phys.*, 1997, **69**, 865; D. T. Papageorgiou, *Phys. Fluids*, 1995, **7**, 1529.
15 (a) J. T. Wang, J. Wang and J. J. Han, *Small*, 2011, **7**, 1728; (b) E. M. Chan, A. P. Alivisatos and R. A. Mathies, *J. Am. Chem. Soc.*, 2005, **127**, 13854.
16 (a) P. Anzenbacher and M. A. Palacios, *Nat. Chem.*, 2009, **1**, 80; (b) L. L. Xu, C. F. Wang and S. Chen, *Angew. Chem. Int. Ed.*, 2014, **126**, 4069.
17 J. Wang, C. F. Wang, H. X. Shen and S. Chen, *Chem. Commun.*, 2010, **46**, 7376.
18 (a) L. K. Yeung and R. M. Crooks, *Nano. Lett.*, 2001, **1**, 14; (b) L. Zhang, L. T. Ling, C. F. Wang, S. Chen, L. Chen and D. Y. Son, *J. Mater. Chem. C.*, 2014, **2**, 3610.
19 L. L. Yan, Z. Y. Yu, L. Chen, C. F. Wang and S. Chen, *Langmuir*, 2010, **26**, 10657.
20 (a) J. Wang, C. F. Wang and S. Chen, *Angew. Chem. Int. Ed.*, 2012, **51**, 9297; (b) X. Guo, C. F. Wang, Z. Y. Yu, L. Chen and S. Chen, *Chem. Commun.*, 2012, **48**, 2692.
21 (a) A. B. Bourlinos, A. Stassinopoulos and D. Anglos, *Chem. Mater.*, 2008, **20**, 4539; (b) Y. X. Zhang, H. Goncalves, J. C. G. Esteves da Silva and C. D. Geddes, *Chem. Commun.*, 2011, **47**, 5313.
22 (a) S. S. Liu, C. F. Wang, X. Q. Wang, J. Zhang, Y. Tian, S. N. Yin and S. Chen, *J. Mater. Chem. C*, 2014, **2**, 9431; (b) H. L. Cong, B. Yu, J. G. Tang, Z. J. Lia and X. S. Liu, *Chem. Soc. Rev.*, 2013, **42**, 7774; (c) Y. J. Zhao, Z. Y. Xie, H. C. Gu, C. Zhu and Z. Z. Gu, *Chem. Soc. Rev.*, 2012, **41**, 3297.
23 W. W. Yu, L. Qu, W. Guo and X. Peng. *Chem. Mater.,* 2003, **15**, 2854.